Climatic conditions for modelling the Northern Hemisphere ice sheets throughout the ice age cycle

A. Abe-Ouchi, T. Segawa, F. Saito

**Climate
of the Past
Discussions**

Climate of the Past Discussions is the access reviewed discussion forum of *Climate of the Past*

CPD

3, 301–336, 2007

**Climatic conditions
for Northern
Hemisphere ice
sheets**

A. Abe-Ouchi et al.

Climatic conditions for modelling the Northern Hemisphere ice sheets throughout the ice age cycle

A. Abe-Ouchi[1,2], T. Segawa[2], and F. Saito[2]

[1]Center for Climate System Research, University of Tokyo, 5-1-5 Kashiwanoha, Kashiwa, 277-8568, Japan
[2]Frontier Research Center for Global Change/Japan Agency for Marine-Earth Science and Technology, 3173-25 Showamachi, Kanagawa, 236-0001, Japan

Correspondence to: A. Abe-Ouchi (abeouchi@ccsr.u-tokyo.ac.jp)

Title Page	
Abstract	Introduction
Conclusions	References
Tables	Figures
◄◄	►►
◄	►
Back	Close
Full Screen / Esc	

Printer-friendly Version

Interactive Discussion

EGU

Abstract

The ice sheet-climate interaction as well as the climatic response to orbital parameters and atmospheric CO_2 content are examined in order to drive an ice sheet model throughout an ice age cycle. Feedback processes between ice sheet and atmosphere are analyzed by numerical experiments using a high resolution General Circulation Model (GCM) under different conditions at the Last Glacial Maximum. Among the proposed processes, the ice albedo feedback, the elevation-mass balance feedback and the desertification effect over ice sheet were found to be the dominant processes for the ice-sheet mass balance. The temperature lapse rate over the ice sheet is proposed to be about $5\,^\circ\mathrm{C\,km^{-1}}$, which is weaker than assumed in other studies. Within the plausible range of parameters related to these processes, the ice sheet response to orbital parameters and atmospheric CO_2 content for the last glacial/interglacial cycle was simulated in terms of both ice volume and geographical distribution, using a three-dimensional ice-sheet model. Careful treatment related to climate-ice sheet feedback is essential for a reliable simulation of ice sheet changes during ice age cycles.

1 Introduction

The climate change during the past 500 000 years is characterized by the wax and wane of the Northern hemisphere ice sheets with a periodicity of about 100 thousand years (kyr), known as glacial and interglacial cycles or ice age cycles (Imbrie et al., 1993). Especially for the Last Glacial Maximum (LGM), not only the total ice volume but also the maximum extent of the Northern Hemisphere ice sheets, such as Laurentide and Fenno-Scandian ice sheets, are well constrained by observational data (Clark and Mix, 2002; Dyke et al., 2002; Svendsen et al., 2004; Peltier, 1994, 2004). To explain why the ice sheets in the Northern Hemisphere grew to the size and extent as observed, and why they retreated quickly at the termination of each 100 kyr cycle is still a challenging theme (Berger et al., 1998; Paillard, 1998; Paillard and Parrenin, 2004).

Although it is now broadly accepted that the orbital variations of the Earth are important for the climatic changes (Milankovitch, 1930; Berger, 1978; Hays et al., 1976), the large amplitude of the ice volume changes and the geographical extent need to be explained by comprehensive models which include nonlinear mechanisms of ice sheet dynamics (Raymo, 1997; Tarasov and Peltier, 1997b; Paillard, 2001; Raymo et al., 2006). Moreover, it is important to explain the geographical extent of the ice sheets, because it has a substantial influence on the climate and the ice sheet itself. Several studies using simple atmospheric models or General Circulation Models (GCMs) have shown that the high albedo and the high altitude of ice sheets can change the temperature, precipitation and the atmospheric circulation over broad spatial scales (Manabe and Broccoli, 1985; Shinn and Barron, 1989; Felzer et al., 1996; Cook and Held, 1998; Krinner and Genthon, 1999; Kageyama and Valdes, 2000; Roe and Lindzen, 2001).

Several studies with ice sheet models have been conducted to simulate the extent of Northern Hemisphere ice sheets at the Last Glacial Maximum and/or its change during the glacial - interglacial cycle. Although it is straightforward, the direct coupling between the sophisticated climate model such as GCM and ice sheet model is still computationally costly and prohibitive. There are three types of alternative approaches to set up climatic conditions for the past and to drive the model of the Northern Hemisphere ice sheets. The first type deals with the ice sheet change between the glacial and interglacial stage using simple climate models driven by orbital forcings and the change of atmospheric content of carbon dioxide (Deblonde and Peltier, 1991; Marsiat, 1994; Tarasov and Peltier, 1997a,b; Tarasov, L. and Peltier, 1999; Charbit et al., 2005). With this approach, the mechanism of ice sheet changes can be studied, while the effects of ignoring of several processes included in GCMs are not clear. The second type is forcing the ice sheet model with time slice experiments with a GCM or a simpler climate model at given time periods such as the LGM or the glacial inception at about 115 thousand years before present (kaBP) (Verbitsky and Oglesby, 1992; Schlesinger and Verbitsky, 1996; Thompson and Pollard, 1997; Fabre et al., 1997, 1998; Ramstein et al., 1997; Huybrechts and T'siobbel, 1997; Pollard and PMIP Participating Groups,

Climatic conditions for Northern Hemisphere ice sheets

A. Abe-Ouchi et al.

Title Page

Abstract	Introduction
Conclusions	References
Tables	Figures

|◄ | ►|

◄ | ►

Back | Close

Full Screen / Esc

Printer-friendly Version

Interactive Discussion

2000; Yamagishi et al., 2005). This approach aims at investigating the possibility of the maintenance or existence of Northern Hemisphere ice sheets, while the climatic changes are not considered. The third type deals with ice sheet changes for a given period (e.g. for one ice age cycle or for the deglaciation period since the LGM) by using time slice experiments of climate models at LGM and present-day and interpolating the climatic field between the two time slices by using the time series of oxygen isotope data of ice cores from Greenland (Huybrechts and T'siobbel, 1995; Greve et al., 1999; Marshall et al., 2000, 2002; Marshall and Clark, 2002; Charbit et al., 2002; Zweck and Huybrechts, 2005). With this approach, the transient behavior of ice sheets and the influence of the climate on it can be examined in detail. However, the ultimate cause of the ice sheet changes cannot be identified with this method because the paleoclimatic data such as the oxygen isotope from ice core is used to drive the ice sheet model.

In this study, we reexamine the climatic factors that control the ice sheet changes with several experiments using a GCM. Critical parameters often assumed in ice sheet model such as lapse rate are also examined. Based on the examination of climatic factors, we present a new method for ice sheet models to study the impact of orbital parameters and atmospheric CO_2 content upon the change of Northern Hemisphere ice sheets. The climate and the ice sheet models used in the study are introduced in Sect. 2. In Sect. 3, the experimental setup is presented and the influence of the ice sheets on the climatic conditions through the albedo feedback, the elevation-mass balance feedback and the stationary wave feedback (Cook and Held, 1998) are discussed. Here we focus on the feedbacks related to temperature since the processes related to precipitation over ice sheets were presented in Yamagishi et al. (2005) (hereafter YASSN05). The influence of orbital parameters and atmospheric CO_2 on climate is briefly examined at the end of Sect. 3. The experimental design and the result of the runs for the past 120 kyr using an ice sheet model are presented and discussed in Sect. 4 and the conclusions are summarized in Sect. 5.

Climatic conditions for Northern Hemisphere ice sheets

A. Abe-Ouchi et al.

Title Page

Abstract | Introduction

Conclusions | References

Tables | Figures

◄◄ | ►►

◄ | ►

Back | Close

Full Screen / Esc

Printer-friendly Version

Interactive Discussion

EGU

2   Model description

2.1   Climate Model

In order to examine the response of climate to the orbital parameters, CO_2 and to ice sheets, a General Circulation Model developed at Center for Climate System Research (CCSR) and National Institute for Environmental Studies (NIES), called CCSR/NIES AGCM5.4 is used (Numaguti et al., 1997). The model was also used for LGM studies and intercomparison of climate at 6 ka and LGM lead by Paleoclimate Modelling Intercomparison Project (PMIP) and also for IPCC Third Assessment Report (TAR). This AGCM coupled with an OGCM was developed as MIROC3.2 (K-1 model developers, 2004) and applied for global warming experiments used in IPCC Assessment Report 4 (AR4) and PMIP2. The model resolution used in the present study is T106, 20 sigma levels vertically as well as T42, 11 levels. The model includes the cumulus parameterization, cloud-radiation interactions, and surface processes. The detailed description is given by Numaguti et al. (1997) and Emori et al. (1999).

2.2   Ice sheet model

The numerical ice-sheet model in this paper, called *IcIES* (Ice sheet model for Integrated Earth system Studies), is almost the same as that described in Saito and Abe-Ouchi (2004), except that it reprojected on the spherical grid system as used in YASSN05. It couples the ice-sheet dynamics to the surface mass balance and the bedrock deformation as explained below.

2.2.1   Ice sheet and bedrock deformation

The ice-sheet dynamic routine computes the evolution of ice thickness and temperature in the shallow ice approximation (Hutter, 1983) including thermodynamics which relates flow velocity and temperature. The model only computes the evolution of grounded ice but not floating ice shelves. The ice sheet model is tested on the present Greenland

Climatic conditions for Northern Hemisphere ice sheets

A. Abe-Ouchi et al.

Title Page

Abstract   Introduction

Conclusions   References

Tables   Figures

◄   ►

◄   ►

Back   Close

Full Screen / Esc

Printer-friendly Version

Interactive Discussion

EGU

and Antarctic ice sheets (Saito and Abe-Ouchi, 2004, 2005). The basic part of the model used in the present paper is almost the same as that used in Saito and Abe-Ouchi (2005). The main difference from the the model used in Saito and Abe-Ouchi (2005, 2004) are the parameterization of basal sliding and the treatment of the temperature field in the bedrock.

The sliding velocity is related to the gravitational driving stress according to Payne (1999),

$$\boldsymbol{v}_B = -A_s \left[\rho_I g H \nabla_H h \right] \ . \tag{1}$$

The parameter A_s is set at $0.01\,\mathrm{m\,yr^{-1}\,Pa^{-1}}$, which corresponds to the maximum value in the sensitivity studies presented in Marshall et al. (2002). Basal sliding is assumed to occur only when the basal ice is at the pressure melting point. The temperature distribution of the lithosphere is considered as in Greve (1997):

$$\frac{\partial T}{\partial t} + \frac{\partial b}{\partial t}\frac{\partial T}{\partial z} = \frac{k_R}{\rho_R c_R}\frac{\partial^2 T}{\partial z^2} \ , \tag{2}$$

where $k_R=3.0\,\mathrm{W\,m^{-1}\,K^{-1}}$ is the heat conductivity of the lithosphere, $\rho_R = 2700\,\mathrm{kg\,m^{-3}}$ is the density of the lithosphere and $c_R=1000\,\mathrm{J\,kg^{-1}\,K^{-1}}$ is the specific heat of the lithosphere. Thickness of the upper lithosphere layer accounted for by the model is set at $5\,\mathrm{km}$ constant (Greve, 1997). The geothermal heat flux at the bottom of the lithosphere is set at a constant value of $42\,\mathrm{mW\,m^{-2}}$ in all experiments. Changes in the glacier bed elevation are calculated by an equation expressing local isostatic rebound:

$$\frac{\partial b}{\partial t} = \frac{1}{\tau_b}\left(b - e + \frac{\rho_I}{\rho_M} H \right) , \tag{3}$$

where $\rho_M = 3300\,\mathrm{kg\,m^{-3}}$ is density of the mantle, and e is the prescribed equilibrium elevation of bedrock with no ice loading, which is obtained with the assumption that the present condition is in an equilibrium. The time constant for isostatic rebound, τ_b, is set

EGU

at 5000 years in the present paper (Tarasov and Peltier, 1997b; Marshall et al., 2000). Hudson bay is treated as land toward which the ice sheet is allowed to advance.

The semi-implicit scheme (Hindmarsh and Payne, 1996) is applied for solving the mass balance equation. The over-implicit scheme (Hindmarsh, 2001; Greve et al., 2002) with the coefficient 1.5 (the weighting factor for the flux at the next time step when solving the mass balance equation) is adopted.

2.2.2 Surface mass balance model

Surface mass balance is parameterized by a Positive Degree-Day (PDD) method (Reeh, 1991), which is used as input of the ice-sheet model. This method relates ablation to both air temperature and snow accumulation. The amount of melting is computed as the product of the number of positive degree days and the PDD factor obtained by observations. It considers the possibility for melting even if the average daily temperature is below the freezing point, different melt rates for snow and ice due to the difference in the albedo Braithwaite and Olesen, 1989), production of superimposed ice and warming created by the phase change. This method is adopted in most numerical studies with ice sheet models (Ritz et al., 1997; Greve, 2000; Huybrechts et al., 2002). In this study, the PDD factor for snow melting is set at $3\,\mathrm{mm\,day^{-1}\,K^{-1}}$ water equivalent following Braithwaite (1995) and Huybrechts et al. (1991), and that for ice melting is set at $8\,\mathrm{mm\,day^{-1}\,K^{-1}}$ water equivalent following Reeh (1991) and Huybrechts et al. (1991). Standard deviation of the daily temperature is assumed as 5 K. It is assumed that 60 % of melt snow refreezes onto superimposed ice. Van de Wal (1996) shows that the PDD method and energy balance method yields very similar results.

Accumulation rate is parameterized partly based on the method presented by Marshall et al. (2002) as follows:

$$A_{cc} = A_{\mathrm{ref}} \times (1 + d_{\mathrm{P}})^{\Delta T_s} \,, \tag{4}$$

where A_{ref} is a reference accumulation, d_{P} is temperature aridity, and ΔT_s is the difference in surface temperature to the reference state. Contrary to Marshall et al. (2002),

Title Page

Abstract | Introduction

Conclusions | References

Tables | Figures

◄ | ►►

◄ | ►

Back | Close

Full Screen / Esc

Printer-friendly Version

Interactive Discussion

EGU

the accumulation lapse rate (elevation-accumulation feedback) is neglected.

The surface temperature, which is used as input for both ice-sheet and surface mass balance models, is parameterized as follows:

$$T_s = T_{ref} + \Delta T_{ice} + \Delta T_{co2} + \Delta T_{insol} + \Delta T_{nonlinear} \cdot \qquad (5)$$

where T_{ref} is the reference temperature, ΔT_{ice} denotes the effect of total atmospheric response to changes in ice sheet size, ΔT_{co2} is the change in temperature according to change in content of atmospheric CO_2, ΔT_{insol} is the change in temperature according to changes in insolation. Each term is described and tested in Sect. 3.

2.2.3 Model set-up

Ice-sheet thickness, bedrock deformation and surface mass balance are computed on the same grid-system on the spherical coordinates. The horizontal model domain spans from 30° N to 89° N and 360° in longitudinal direction with periodical boundary conditions. The horizontal grid resolution is 1° in the both coordinate directions. The vertical grid is divided into 26 levels. The model time step is 2 years.

3 Evaluation of climatic condition for ice sheet by GCM

The main focuses in this section are on the relative contribution to the climatic condition over ice sheet of: (a) ice sheet itself, (b) orbital parameters and (c) atmospheric CO_2 content. Moreover, the contribution of ice sheet itself to climate is through the high ice albedo and the high and massive ice topography. Since a GCM is used to evaluate the climatic condition in this study, the cloud feedback and water vapor feedback are included already in the evaluation of the climatic condition that we discuss. It is not attempted to separate from each other or from the effects of ice sheet itself, orbital parameters and CO_2 content.

Climatic conditions for Northern Hemisphere ice sheets

A. Abe-Ouchi et al.

EGU

The climatic contribution for ice sheet modeling is mainly temperature and precipitation, which are the practical input for the ice sheet model as in other studies. In this study, the northern hemispheric summer temperature is analyzed, since the surface ice melting of the northern ice sheets is primarily determined by the summer temper-
5　ature in June, July and August (Ohmura, 2001). The precipitation over ice sheets and its relation to temperature was presented in the YASSN05 paper. Thus, we limit the discussion on the precipitation over ice sheets to the end of Sect. 3.2.

3.1　Experimental design

A total of 19 experiments, summarized in Table 1, were designed to study the factors
10　that determine the surface temperature over ice sheets. Three groups of experiments were performed as follows.

The first group uses a high resolution (T106, 1.1° in latitude and longitude) atmospheric GCM with fixed sea surface temperature (SST) for the study of the ice sheet-atmosphere interaction. Experiments named CTLH and LGMfull are based on the pro-
15　tocol of The Paleoclimate Modelling Intercomparison Project (PMIP; Joussaume and Taylor, 1995), where CTLH represents a present day control simulation and LGMfull is the LGM experiment. CLIMAP data (CLIMAP, 1981) is used for the SST, data from Peltier (1994) is applied for ice-sheet topography and extent. Insolation parameters are set at the LGM values and the CO_2 content is set at 200 ppm. LGMflat is a sensitivity
20　experiment, where the ice sheet covers the same area as in LGMfull but the thickness is set to 0 m except for Greenland and Antarctica, for which the present topography is taken. The distribution of surface albedo and other parameters is set the same as in LGMfull. In the LGMnice experiment, the ice sheet and SST are the same as in CTLH, while CO_2 and insolation parameters are set the same as in LGMfull. Each experiment
25　is run for 11 or 13 model years, and the results for the last 10 years are used for the analysis. The computation time for one experiment was about 40 days per 10 model years on an NEC SX-5 with a single processor.

The second group of experiments is designed to examine the dependence of climatic

Climatic conditions for Northern Hemisphere ice sheets

A. Abe-Ouchi et al.

Title Page

Abstract　　Introduction

Conclusions　　References

Tables　　Figures

|◄　　►|

◄　　►

Back　　Close

Full Screen / Esc

Printer-friendly Version

Interactive Discussion

EGU

conditions on the size of the ice sheets. Similar experiments as in the first group were performed but with a different size of the ice sheets, however, leaving other conditions the same as given in Table 1. Among the ICE-4G (Peltier, 1994) time slices, the ice sheet size at 12 ka was chosen since its area is about half of the LGM size. A medium resolution, (T42, latitude and longitude $2.8°$ for horizontal and 11 layers mainly in the troposphere for vertical resolution) is used for the experiments for saving CPU-time compared to the first group experiment, but the slab ocean model is used to take into account the thermal feedback of the oceans. These experiment are called M21nice, M21flat, M12nice, M12flat and M0CTL. Each experiment was run for 50 model years, and the results for the last 10 years are used for the analysis.

The third group of experiment is designed to separate the influence of the atmospheric CO_2 content and the orbital parameter. Extreme situations due to (1) different precession combined with large eccentricity and (2) extreme obliquities were chosen to examine the range of climatic condition due to different orbital parameters during the late Quaternary. CO_2 levels of 200, 280, 345 ppm are examined combined with different orbital parameters and existence of ice sheets are chosen as given in Table 1. These experiments are called MyOlCk, where y, l and k denote the ice sheet distribution, the orbital condition and CO_2 content, respectively. A medium resolution climate model with slab ocean was used.

3.2 Ice sheet-atmosphere feedback

The effect of the ice sheet itself and the other effects upon the cooling are compared for summer surface air temperature (mean of June, July and August) obtained by the experiments LGMfull, LGMnice, and CTLH. The total cooling by the ice sheet itself is given by the difference LGMfull–CTLH, Fig. 1a. Compared to this, the cooling due to other effects such as the CO_2 effect, orbital effect and the effect due to the difference in SST, LGMnice–CTLH, is shown in Fig. 1b. The cooling in Fig. 1a is much larger than that in Fig. 1b over the ice sheet region. Therefore, the cooling due to the existence alone of large ice sheets at LGM is the dominant effect which should be treated

EGU

separately.

For the influence of ice sheet itself, the high albedo and the high altitude of ice sheet can be both important. LGMflat–LGMnice and LGMfull–LGMflat will be here assumed to be the high albedo effect (flat ice sheet effect) and ice topography effect, respectively. For the ice topography effect, one could be a 'local' effect, while the other could be a 'non-local' effect. A well known 'local' ice topography effect is the so-called "lapse rate effect", which causes cooling over the ice sheet just because of the locally high altitude. This was also addressed in Krinner and Genthon (1999) for the case of Antarctica by changing its surface elevation in the GCM. The 'non-local' topography effect can be important through the influences upon the atmospheric circulation and/or cloud distribution (Shinn and Barron, 1989; Felzer et al., 1996; Cook and Held, 1998). Altogether the ice sheet itself is separated in three categories, flat ice effect, lapse-rate effect and topography effect other than lapse rate effect (as a residual), which correspond to (c), (d), (e) in Fig. 1, respectively. For the lapse rate effect, a lapse rate of $5\,\mathrm{K\,km^{-1}}$ was assumed. The summation of (b), (c), (d), (e) is equal to (a).

In order to examine the "lapse rate" in the model, the cooling due to the topography, namely LGMfull–LGMflat is plotted for the change of altitude for all grid points in the ice sheet area of this high resolution GCM as in Fig. 2. The relation of $5\,^{\circ}\mathrm{C}$ cooling per 1 km altitude change is shown as a red line. Although there is a large scatter, it is seen that the temperature drops as the altitude increases. Other lapse rate can be also assumed depending on the altitude or location, while lapse rate larger than $7\,\mathrm{K\,km^{-1}}$ or smaller than $4\,\mathrm{K\,km^{-1}}$ deviates the overall feature. This is consistent with the finding of Krinner and Genthon (1999), who suggest a lapse rate of $5.5\,\mathrm{K\,km^{-1}}$, which contrasts conventional studies generally using lapse rates of $8\,\mathrm{K\,km^{-1}}$ or $6.5\,\mathrm{K\,km^{-1}}$ to drive the ice sheet models (e.g. Fabre et al., 1997, 1998; Ramstein et al., 1997; Huybrechts and T'siobbel, 1997; Pollard and PMIP Participating Groups, 2000; Tarasov and Peltier, 1997a,b; Tarasov, L. and Peltier, 1999; Charbit et al., 2005; Greve et al., 1999; Marshall and Clark, 2002; Marshall et al., 2000, 2002; Charbit et al., 2002; Zweck and Huybrechts, 2005). In Fig. 2, the temperature change due to a change of remote

ice sheets as well as the local ice sheet is included, as shown with the relative low temperature change over the Greenland ice sheet (red) or some part of Laurentide ice sheet (black) compared to Fennoscandian ice sheet (blue). The overall geographical pattern of the scatter outside of a line (red line) corresponds to Fig. 1e. Except the region around Greenland and the north-east side of Laurentide ice sheet, the residuals shown in Fig. 1e are small compared to the albedo effect shown in Fig. 1c or lapse rate effect shown in Fig. 1d.

The temperature difference in Fig. 1e must be related to an atmospheric circulation effect such as the "Stationary wave effect" studied in Cook and Held (1998). To examine the stationary waves in our model, the summer geopotential height difference at 500 hPa level due to ice sheet topography, LGMfull−LGMflat, is shown in Fig. 1f. The surface topography induces higher height on the west side of Laurentide sheet and lower height in the east. Around the Fennoscandian ice sheet, a series of wave pattern from east to west seems to be influenced by both large ice sheets in the Northern Hemisphere. Its pattern is similar to the pattern in the surface temperature changes in Fig. 1d, which is consistent with the findings of Cook and Held (1998).

The result of ice sheet effect seems to be dependent on the size of the ice sheet. Figure 3 shows the flat ice sheet effect for 12 ka ice sheet size and LGM ice sheet size. As a result, the larger the ice sheet size is, the larger the cooling is. The cooling over ice sheet is larger than 15 K for the LGM ice, and the cooling over the flat ice sheet is largely distinctive compared to the cooling outside the ice sheet. Since the climate model is now a slab mixed layer ocean model, the cooling due to the ice sheet itself outside the ice sheet is also seen.

For the summer temperature over the ice sheet, the dominant effect is the albedo effect and lapse rate effect shown in Figs. 1c and d, respectively. The effect due to the stationary wave effect shown in Fig. 1e is a secondary effect compared to the albedo and lapse rate effects. The area dependence of albedo effect should be taken into account, and the lapse rate is about $5\,\mathrm{K\,km^{-1}}$, which is weaker than the conventional value. The implication is that the size dependent albedo effect should be taken into ac-

count and a weaker lapse rate than suggested by previous studies should be assumed for the ice sheet modeling.

Finally, it is important to consider whether the result is model dependent, although this should be investigated in detail as a future topic. Figure 4 shows the recent result
5 of some PMIP2 models (in PMIP2 database in April, 2006), which are summer cooling in the same domain as in Fig. 2 and Fig. 3, but reducing the total cooling (LGM minus present day) by assuming a constant lapse rate using the topography in each model. Clear distinctive cooling over ice sheet is still seen, while the strength of cooling depends on the model. HadCM3M2 has the strongest cooling, while the CCSM has
10 the weakest cooling over ice sheet especially for Fennoscandian ice sheet. This is not necessarily correlated to the whole globe. It could be partly due to the different albedo feedback and different cloud feedback, which largely determine the climate sensitivity in each model. Slightly different response in atmospheric circulation such as the stationary wave or the position of storm track and ocean circulation such as the response
15 of meridional overturning in the North Atlantic or the position of Gulf Stream could also lead to the different cooling over the ice sheet in the three models. Therefore the albedo effect for flat ice sheet here should be taken with some range of uncertainty.

The precipitation over ice sheets and its relation to temperature was studied in the YASSN05 paper. Here we discuss the results of three different GCMs of the PMIP2
20 in relation to precipitation. Figure 5 shows the annual precipitation change ratio in per cent, which can be compared to the result of Fig. 1 of YASSN05. Overall feature shows the larger desertification effect in the inland of ice sheet and for cooler temperature. The model with larger cooling sensitivity as in HadCM3 compared to other models also show a larger precipitation drop, which is even more than 80% and this is consistent
25 with the previous finding in YASSN05. What is not seen in these PMIP2 runs is the precipitation increase in the south-east margin of Laurentide ice sheet at LGM ,which was seen in YASSN05 and also discussed in previous studies as in Kageyama and Valdes (2000). This demonstrates that a resolution of 2.5 to 3 degree in latitude and longitude in the used GCMs is not good enough to produce an accurate input for precipitation for

Climatic conditions for Northern Hemisphere ice sheets

A. Abe-Ouchi et al.

Title Page

Abstract | Introduction

Conclusions | References

Tables | Figures

◄◄ | ►►

◄ | ►

Back | Close

Full Screen / Esc

Printer-friendly Version

Interactive Discussion

EGU

the south-east margin of the ice sheet for driving ice sheet models.

3.3   Response of climate to orbital parameters and CO_2

Response of climate to orbital parameters and CO_2 were examined in both cases with ice sheet and without ice sheet as in Table 1. Figures 6a and c show an example of response to precessional condition by M21O1C1 minus M21O2C1, and Figs. 6b and d show the response to change in CO_2 by M21O1C1 minus M21O1C3 for the response of 3 months temperature (June, July, August and December, January and February). In both cases there is a larger response over the land than over the ocean except over sea ice region. Also there is a larger response for orbital effect than the CO_2 effect in this model. Later the ice sheet model is driven by the orbital effect and CO_2 effect based on this estimation over land in the Northern Hemisphere. Again the cloud feedback and water vapor feedback are included in the response, and this might result in the different sensitivity for ice sheet change.

Non-linear effect due to the combined orbital, CO_2 and even ice sheet effect was checked by examining other combinations as in Table 1. Although this will be discussed in more detail in a separate paper in future, the nonlinear effect was at most about 15% and no more than 20%. Since, in general, the response is larger under cooler climate, the same change in CO_2 or orbital parameters can result in a slightly larger response with ice sheet than without ice sheet. This should be taken into account in future, although omitted in Sect. 4 for simplicity.

4   Ice sheet model experiments with GCM information

The main focus of this section is to use the GCM results obtained in the previous section for forcing an ice sheet model for one glacial-interglacial cycle. Instead of using geographically distributed information, we use spatially uniform climatic input for the ice sheet model in the first step. The system is driven by a combination of orbital

Title Page

Abstract   Introduction

Conclusions   References

Tables   Figures

◄   ►

◄   ►

Back   Close

Full Screen / Esc

Printer-friendly Version

Interactive Discussion

EGU

(Milankovitch) and CO_2 forcings. We investigate whether the main features of glacial-interglacial cycles, such as the fast retreat of ice sheets at the termination and the geographical pattern is properly simulated at key periods such as the LGM. Several runs are performed to investigate the sensitivity of the results to the parameters in
5 realistic ranges of values.

4.1   Experimental set-up of the ice sheet model

4.1.1   Standard experimental setup

The IcIES ice sheet model described in Sect. 2.2 is used for the glacial-interglacial experiments. The forcing scenarios are incorporated into the terms ΔT_{co2} and ΔT_{insol}
10 in Eq. (5), which are prescribed without feedback from ice-sheets.

The time series of CO_2 content obtained from Vostok ice core (Petit et al., 1999) is applied. Changes in temperature due to change in CO_2 content are parameterized using the following relation:

$$\Delta T_{co2} = \frac{\frac{C}{240} - 1}{\frac{280}{240} - 1} \times 1.088 - 1.81584 \qquad (6)$$

where C is the atmospheric content of CO_2 in ppm. This relation is derived from the AGCM experiments in the present paper.

To obtain the effect of changes in insolation, we first compute time series of July insolation at 65° N, using the orbital parameters in Berger (1978). Then change in temperature due to change in the insolation is parameterized using following relation estimated from our GCM runs in the previous section:

$$\Delta T_{insol} = \frac{Q - 440}{480 - 440} \times 3.25 + 1.0757 \;, \qquad (7)$$

where Q is the insolation in $W\,m^{-2}$.

315

Title Page

Abstract | Introduction

Conclusions | References

Tables | Figures

◀◀ | ▶▶

◀ | ▶

Back | Close

Full Screen / Esc

Printer-friendly Version

Interactive Discussion

EGU

The other terms in Eq. (5) are also derived from the AGCM experiments. We assume in this study that the non-linearity $\Delta T_{nonlinear}$ is zero, although it can be up to 20% as explained in Sect. 3.3. This contribution will be included in the following ice sheet effect.

We divide the ice-sheet effect ΔT_{ice} on the surface temperature in two terms as follows:

$$\Delta T_{ice} = \Delta T_{elv} + \Delta T_{area} \tag{8}$$

where ΔT_{elv} the effect of change in surface elevation, and ΔT_{area} denotes the effect of albedo change.

The lapse-rate effect ΔT_{elv} is a function of ice-sheet elevation as follows:

$$\Delta T_{elv} = \lambda(h - h_{ref}) \,, \tag{9}$$

where h_{ref} is the reference ice-sheet elevation.

The albedo effect ΔT_{area} is assumed to be a function of the ice-sheet area A_{rea},

$$\Delta T_{area} = \max\left[\Delta T_{area}^{min}, \Delta T_{area}^{0} + \gamma_{area}^{T} \times A_{rea}\right] \,. \tag{10}$$

We assume a linear dependence on temperature with three coefficients, prescribed minimum albedo effect ΔT_{area}^{min}, offset of albedo effect ΔT_0^{min} and dependence of albedo effect on the ice-sheet cover γ_{area}.

For the choice of the parameters in Eqs (9) and (10), we perform sensitivity experiments, which will be explained in Sect. 4.1.2.

For the reference temperature distribution, we apply the climatology of present day, obtained from ERA40 (re-analysis of the European Centre for Medium-Range Weather Forecast).

In addition, temperature aridity d_P in Eq. (4) is also derived from the AGCM experiments in YASSN05 paper. Contrary to Marshall et al. (2002), the temperature aridity d_P is assumed as a function of ice-sheet area as follows:

$$d_P = \min\left[d_0 \times \frac{A_{rea}}{1.4 \times 10^{13}}, 1.0\right] \,, \tag{11}$$

316

where A_{rea} is the area covered by ice-sheet in m^2 unit. The reference area $1.4 \times 10^{13} \, m^2$ approximately corresponds to that of Laurentide ice sheet at the last glacial maximum of Peltier (1994).

The total model domain in this study is divided into four parts: North America, Eura-
5 sia, Greenland and elsewhere. A_{rea} used Eqs. (10) and (11), is computed in each part as the sum of the area of all grid cells where ice exists.

The time integration is performed for the last 120 thousand years in the present paper. For the initial conditions, we take a situation which is close to the present day condition, as shown in Fig. 7a from one of our experiments of longer time integration.
10 Several initial conditions at 130 kaBP and before are examined (not shown). It is found, however, that the difference in the initial conditions is small and does not affect the results for the last 120 ka.

4.1.2 Experimental set-up of the sensitivity studies

In order to study influences from uncertain processes on the response of ice sheet to
15 climate change, several sensitivity experiments were performed. In this paper, sensitivity experiments to the choice of the lapse-rate, albedo effect and the desertification rate are shown. The parameters are summarized in Table 2.

The lapse rate λ in Eq. (9) is set at $-5.0 \, K \, km^{-1}$ as the standard value, but sensitivity experiments with different values such as $-4.0 \, K \, km^{-1}$ and $-6.0 \, K \, km^{-1}$ were carried
20 out.

The desertification rate parameter, corresponding to d_0 in Eq. (11), is set at 0.022 as the standard value, which is obtained from YASSN05. We also performed sensitivity studies with a smaller $d_0 = 0.01$ and a larger $d_0 = 0.04$.

In the standard configuration, coefficients in Eq. (10) are set as $\Delta T_{area}^{min} =$
25 $-13.0 \, K$, $\Delta T_0^{min} = -4.0 \, K$ and $\gamma_{area} = -4.7 \times 10^{-13} \, K \, m^{-2}$. We performed sensitivity studies on the temperature-dependence coefficient γ_{area} with two cases, $\gamma_{area} = -3.7 \times 10^{-13} \, K \, m^{-2}$ and $\gamma_{area} = -5.7 \times 10^{-13} \, K \, m^{-2}$.

Title Page

Abstract | Introduction

Conclusions | References

Tables | Figures

◄◄ | ►►

◄ | ►

Back | Close

Full Screen / Esc

Printer-friendly Version

Interactive Discussion

EGU

4.2 Glacial-interglacial experimental results

As for the standard experiment, the result of the altitude distribution of ice sheet is shown in Fig. 7 for various time periods, and the time series are shown in Fig. 8 by black thick lines. The gradual growth and the fast retreat of the ice sheets is the char-
5 acteristics, known as "sawtooth" shape, similar to the proxy data such as SPECMAP (Imbrie et al., 1993). The maximum volume of about 138 meter of sea level equivalent at 15 kaBP is somewhat larger than what is discussed in literature (e.g. Clark and Mix, 2002; Peltier, 2004), but the geographical pattern is quite well simulated as in Fig. 7(d). It well captures the relatively larger Laurentide ice sheet than the Eurasian ice sheet
10 and the merge of the ice sheet over Labrador and the Rockies, which were split in most of the other stages. The Laurentide ice sheet splits before 10 kaBP but the termination is not as complete as observed at present day, and some remnant of ice is left over in the Canadian archipelago and in the Kara Sea. The maximum of the ice volume is somewhat later than reconstructed at 21 ka, known as LGM.
15   Figure 8 shows the results of the sensitivity of the ice volume to the parameters of the albedo effect, temperature lapse rate, and desertification rate. Larger lapse rate or larger albedo effect or smaller desertification effect result in larger ice sheets at about 20 kaBP at the maximum volume stage. In almost all experiments the inception and termination of ice age occur. In almost all cases, the larger ice sheet at the glacial max-
20 imum end with a larger ice left at the 0 kaBP after termination. Extreme combinations of these parameters results in extremely large ice sheets, with volumes up to 300 meters in sea level equivalent. These results demonstrate the importance of careful treatment of parameters related to ice sheet and atmosphere interactions.

4.3 Discussion

25 Although the overall features of the ice sheets are well simulated, some detailed fea-
ture are not captured correctly, such as (1) the remnant ice at 0 kaBP, (2) insufficient growth rate at ice age inception between 120 kaBP and 110 kaBP, (3) overestimated

Climatic conditions for Northern Hemisphere ice sheets

A. Abe-Ouchi et al.

Title Page

Abstract | Introduction

Conclusions | References

Tables | Figures

◀◀ | ▶▶

◀ | ▶

Back | Close

Full Screen / Esc

Printer-friendly Version

Interactive Discussion

EGU

volume of ice sheet and the delay of timing of the glacial maximum and (4) overestima-tion of ice extent of Eurasian ice sheet. These features may come from deficiencies or simplifications or assumptions in the model and experimental setup, such as the omis-sion of possible non-linear effects or assumption of a constant lapse rate or the too

5 simple relation between the albedo feedback and ice sheet size. Additionally the rep-resentation of sub-grid scale phenomena of ice dynamics, omission of feedbacks due to atmospheric circulation such as stationary wave feedback or storm track feedback and other feedbacks from ocean or vegetation should also be considered for future investigation.

10 Uncertainties in ice-sheet modeling such as basal-sliding parameterization, geother-mal heat flux, isostatic response and so on should be investigated as suggested in Marshall et al. (2002); Charbit et al. (2002); Zweck and Huybrechts (2005). Also, sev-eral studies have reported that there are significant errors in the simulated ice thickness near the margin (e.g., Huybrechts et al., 1996). Van den Berg et al. (2006) have shown

15 that these errors are enhanced by the feedback between the surface mass balance and height. They also showed that these errors strongly influence the time scale of the simulated volume changes. The implementation of an improved scheme to reduce the error at the ice margin (Saito et al., in press) is a next step of the present study. The influence of the above uncertainties on the results of the present paper will be

20 addressed in future research.

5 Summary and conclusions

Feedback processes between ice sheets and the atmosphere are analyzed by nu-merical experiments using a high resolution GCM under different conditions at the Last Glacial Maximum. Among the proposed processes, the ice albedo feedback,

25 the elevation-mass balance feedback and the desertification effect over the ice sheets were found to be the dominant processes for the ice-sheet mass balance. The lapse rate over ice sheets is proposed to be $5\,°C\,km^{-1}$, which is smaller than proposed by

other studies. Within a plausible range of parameters related to these processes, the ice sheet response to orbital parameters and atmospheric CO_2 content for the last glacial/interglacial cycle was simulated in terms of both ice volume and geographical distribution, using a three-dimensional ice-sheet model. Since the cooling and the drop

5 in precipitation over the ice sheets depends on the parameterizations in the models, a careful treatment of the processes related to atmosphere-ice sheet feedback is essential for the simulation of ice sheet changes during an ice age cycle.

References

Bard, E., Hamelin, B., Arnold, M., Montaggioni, L., Cabioch, G., Faure, G., and Rougerie, F.: A 17 000-year glacio-eustatic sea level record: influence of glacial melting rates on the Younger Dryas event and deep-ocean circulation, Nature, 382, 241–244, 1989.

15 Berger, A.: Long-term variations of caloric insolation resulting from the Earth's orbital elements, Quat. Res., 9, 139–167, 1978. 303, 315

Berger, A., Loutre, M. F., and Gallée, H.: Sensitivity of the LLN climate model to the astronomical and CO_2 forcings over the last 200 ky, Clim. Dyn., 14, 615–629, 1998. 302

Bintanja, R., van de Wal, R. S. W., and Oerlemans, J.: Global ice volume variations through the

20 last glacial cycle simulated by a 3-D ice-dynamical model, Quat. Int., 95–96, 11–23, 2002.

Braithwaite, R. J.: Positive degree-day factors for ablation on the Greenland ice sheet studied by energy-balance modelling, J. Glaciol., 41, 153–160, 1995. 307

Braithwaite, R. J. and Olesen, O. B.: Calculation of glacier ablation from air temperature, West Greenland, in: Glacier fluctuations and climatic change, edited by Oerlemans, J., pp. 219–

25 233, Dordrecht, Kluwer Academic Publishers, 1989. 307

Broccoli, A. J. and Manabe, S.: The influence of continental ice, atmospheric CO_2 and land albedo on the climate of the last glacial maximum, Climate Dyn., 1, 87–99, 1987.

Charbit, S., Ritz, C., and Ramstein, G.: Simulations of Northern Hemisphere ice-sheet retreat:

Climatic conditions for Northern Hemisphere ice sheets

A. Abe-Ouchi et al.

sensitivity to physical mechanisms involved during the Last Deglaciation, Quat. Sci. Rev., 21, 243–265, 2002. 304, 311, 319

Charbit, S., Kageyama, M., Roche, D., Ritz, C., and Ramstein, G.: Investigating the mechanisms leading to the deglaciation of past continental northern hemisphere ice sheets with the CLIMBER-GREMLINS coupled model, Global and Planetary Change, 48, 253–273, doi: doi:10.1016/j.gloplacha.2005.01.002, 2005. 303, 311

Clark, P. U.: Unstable Behavior of the Laurentide Ice Sheet over Deforming Sediment and Its Implications for Climate Change, Quat. Res., 41, 19–25, 1994.

Clark, P. U. and Mix, A. C.: Ice sheets and sea level of the Last Glacial Maximum, Quat. Sci. Rev., 21, 1–7, 2002. 302, 318

CLIMAP: Seasonal reconstructions of the Earth's surface at the last glacial maximum, no. MC-36 in Map Chart Series, Geological Society of America, Boulder, Colorado, 1981. 309

Cook, K. H. and Held, I. M.: Stationary waves of the ice age climate., J. Climate, 1, 807–819, 1998. 303, 304, 311, 312

Deblonde, G. and Peltier, W. R.: Simulations of Continental Ice Sheet Growth Over the Last Glacial-Interglacial Cycle: Experiments With a One-Level Seasonal Energy Balance Model Including Realistic Geography, J. Geophys. Res., 96, 9189–9215, 1991. 303

Deblonde, G. and Peltier, W. R.: Late Pleistocene Ice Age Scenarios Based on Observational Evidence, J. Climate, 6, 709–727, 1993.

Dyke, A. S., Andrews, J. T., Clark, P. U., England, J. H., Miller, G. H., Shaw, J., and Veillette, J. J.: The Laurentide and Innuitian ice sheets during the Last Glacial Maximum, Quat. Sci. Rev., 21, 9–31, 2002. 302

Emori, S., Nozawa, T., Abe-Ouchi, A., Numaguti, A., Kimoto, M., and Nakajima, T.: Coupled ocean-atmosphere model experiments of future climate change with an explicit representation of sulfate aerosol scattering, J. Met. Society Japan, 77, 1299–1307, 1999. 305

Fabre, A., Ritz, C., and Ramstein, G.: Modelling of Last Glacial Maximum ice sheets using different accumulation parameterizations, Ann. Glaciol., 24, 223–228, 1997. 303, 311

Fabre, A., Ramstein, G., Ritz, C., Pinot, S., and Fournier, N.: Coupling an AGCM with an ISM to investigate the ice sheets mass balance at the Last Glacial Maximum, Geophys. Res. Lett., 25, 531–534, 1998. 303, 311

Fairbanks, R. G.: A 17 000-year glacio-eustatic sea level record: influence of glacial melting rates on the Younger Dryas event and deep-ocean circulation, Nature, 342, 637–642, 1989.

Felzer, B., Oglesby, R. J., III, T. W., and Hyman, D. E.: Sensitivity of a general circulation model

Title Page

Abstract | Introduction

Conclusions | References

Tables | Figures

◄ | ►

◄ | ►

Back | Close

Full Screen / Esc

Printer-friendly Version

Interactive Discussion

EGU

to changes in northern hemisphere ice sheets, J. Geophys. Res., 101, 19 077–19 092, 1996. 303, 311

Greve, R.: Application of a polythermal three-dimensional ice sheet model to the Greenland ice sheet: response to steady-state and transient climate scenarios, J. Climate, 10, 901–918, 1997. 306

Greve, R.: On the response of the Greenland ice sheet to greenhouse climate change, Climate Change, 46, 289–303, 2000. 307

Greve, R., Wyrwoll, K.-H., and Eisenhauer, A.: Deglaciation of the Northern hemisphere at the onset of the Eemian and Holocene, Ann. Glaciol., 28, 1–8, 1999. 304, 311

Greve, R., Wang, Y., and Mügge, B.: Comparison of numerical schemes for the solution of the advective age equation in ice sheets, Ann. Glaciol., 35, 487–494, 2002. 307

Hays, J. D., Imbrie, J., and Shackleton, N. J.: Variations in the Earth's orbit: pacemaker of the ice ages, Science, 194, 1121–1132, 1976. 303

Hindmarsh, R. C. A.: Notes on basic glaciological computational methods and algorithms, in: Continuum Mechanics and Applications in Geophysics and the Environment, edited by Straughan, B., Greve, R., Ehrentraut, H., and Wang, Y., pp. 222–249, Springer-Verlag, Berlin, 2001. 307

Hindmarsh, R. C. A. and Payne, A. J.: Time-step limits for stable solutions of the ice-sheet equation, Ann. Glaciol., 23, 74–85, 1996. 307

Hutter, K.: Theoretical glaciology; material science of ice and the mechanics of glaciers and ice sheets, Dordrecht, etc., D. Reidel Publishing company/Tokyo, 1983. 305

Huybrechts, P. and T'siobbel, S.: Thermomechanical modelling of northern Hemispher ice sheets with a two-level mass-balance parameterization, Ann. Glaciol., 21, 111–116, 1995. 304

Huybrechts, P. and T'siobbel, S.: A three-dimensional climate-ice-sheet model applied to the Last Glacial Maximum, Ann. Glaciol., 25, 333–339, 1997. 303, 311

Huybrechts, P., Letréguilly, A., and Reeh, N.: The Greenland ice sheet and greenhouse warming, Palaeogeography, Palaeoclimatology, Palaeoecology, 89, 399–412, 1991. 307

Huybrechts, P., Payne, T., and The EISMINT Intercomparison group: The EISMINT benchmarks for testing ice-sheet models, Ann. Glaciol., 23, 1–12, 1996. 319

Huybrechts, P., Janssens, I., Poncin, C., and Fichefet, T.: The response of the Greenland ice sheet to climate changes in the 21st century by interactive coupling of an AOGCM with a thermomechanical ice-sheet model, Ann. Glaciol., 35, 409–415, 2002. 307

Climatic conditions for Northern Hemisphere ice sheets

A. Abe-Ouchi et al.

Title Page

Abstract | Introduction

Conclusions | References

Tables | Figures

◄ | ►|

◄ | ►

Back | Close

Full Screen / Esc

Printer-friendly Version

Interactive Discussion

EGU

Imbrie, J., Berger, A., Boyle, E. A., Clemens, S. C., Duffy, A., Howard, W. R., Kukla, G., Kutzback, J., Martinson, D. G., McIntyre, A., Mix, A. C., Molfino, B., Morley, J. J., Peterson, L. C., Pisias, N. G., Prell, W. L., Raymo, M. E., Shackleton, N. J., and Toggweiler, J. R.: On the structure and origin of major glaciation cycles. 2. The 100,000-year cycle, Paleoceanography, 8, 699–735, 1993. 302, 318

Jost, A., Lunt, M., Kageyama, M., Abe-Ouchi, A., Peyron, O., Valdes, P. J., and Ramstein, G.: High resolution simulations of the last glacial maximum climate over Europe: a solution to discrepancies with continental paleoclimatic reconstructions?, Clim. Dyn., doi:10.1007/s00382-005-0009-4, 2005.

Joussaume, S. and Taylor, K.: Status of the paleoclimate modeling intercomparison project (PMIP), in: WCRP-2, First International AMIP Scientific Conference, 15–19 May 1995, Monterey, CA. Proceedings, pp. 415–430, Geneva, World Meteorological Organisation. World Climate Research Programme, 1995. 309

K-1 model developers: K-1 Coupled GCM (MIROC) Description, K-1 technical report 1, Center for Climate System Reserach, edited by Hiroyasu Hasumi and Seita Emori, 2004. 305

Kageyama, M. and Valdes, P. J.: Impact of the North American ice-sheet orography on the Last Glacial Maximum eddies and snowfall, Geophys. Res. Lett., 27, 1515–1518, 2000. 303, 313

Krinner, G. and Genthon, C.: Altitude dependence of the ice sheet surface climate, Geophys. Res. Lett., 26, 2227–2230, 1999. 303, 311

Manabe, S. and Broccoli, A. J.: The influence of continental ice sheets on the climate of an ice age, J. Geophys. Res., 90, 2167–2190, 1985. 303

Marshall, S. J. and Clark, P. U.: Basal temperature evolution of North American ice sheets and implications for the 100-kyr cycle, Geophys. Res. Lett., 29, 67, 2002. 304, 311

Marshall, S. J., Tarasov, L., Clarke, G. K. C., and Peltier, W. R.: Glaciological reconstruction of the Laurentide ice sheet: physical processes and modelling challenges, Can. J. Earth Sci., 37, 769–793, 2000. 304, 307, 311

Marshall, S. J., James, T. S., and Clarke, G. K. C.: North American Ice Sheet reconstructions at the Last Glacial Maximum, Quat. Sci. Rev., 21, 175–192, 2002. 304, 306, 307, 311, 316, 319

Marsiat, I.: Simulation of the Northern Hemisphere continental ice sheets over the last glacial interglacial cycle: experiments with a latitude-longitude vertically integrated ice sheet model coupled to a zonally averaged climate model, Paleoclimates, 1, 59–98, 1994. 303

Milankovitch, M.: Mathematische Klimalehre und Astronomische Theorie der Klimaschwankun-

Climatic conditions for Northern Hemisphere ice sheets

A. Abe-Ouchi et al.

EGU

gen, Gebrüder Borntreger, Berlin, 1930. 303

Numaguti, A., Takahashi, T., Nakajima, T., and Sumi, A.: Description of CCSR/NIES atmospheric general circulation model, in: CGER's Supercomputer Monograph Report, vol. 3, Tokyo, National Institute for Environmental Studies, Center for Global Environmental Research, 1997. 305

Ohmura, A.: Physical Basis for the Temperature-Based Melt-Index Method, J. Appl. Meteorol., 40, 753–761, 2001. 309

Paillard, D.: The timing of Pleistocene glaciations from a simple multiple-state climate model, Nature, 391, 378–381, 1998. 302

Paillard, D.: Glacial cycles: toward a new paradigm, Rev. Geophys., 39, 325–346, 2001. 303

Paillard, D. and Parrenin, F.: The Antarctic ice sheet and the triggering of deglaciations, Earth Planet. Sci. Lett., 227, 263–271, 2004. 302

Payne, A. J.: A thermomechanical model of ice flow in West Antarctica, Clim. Dyn., 15, 115–125, 1999. 306

Peltier, W. R.: Ice Age Paleotopography, Science, 265, 195–201, 1994. 302, 309, 310, 317

Peltier, W. R.: Global Glacial Isostasy and the Surface of the Ice-Age Earth: The ICE-5G(VM2) Model and GRACE, Annu. Rev. Earth Planet. Sci., 32, 111–149, 2004. 302, 318

Petit, J. R., Jouzel, J., Raynaud, D., Barkov, N. I., Barnola, J.-M., Basile, I., Bender, M., Chappellaz, J., Davis, M., Delayque, G., Delmotte, M., Kotlyakov, V. M., Legrand, M., Lipenkov, V. Y., Lorius, C., Pépin, L., Ritz, C., Saltzman, E., and Stievenard, M.: Climate and atmospheric history of the past 420 000 years from the Vostok ice core, Antarctica, Nature, 399, 429–436, 1999. 315

Pollard, D. and PMIP Participating Groups: Comparisons of ice-sheet surface mass budgets from Paleoclimate Modeling Intercomparison Project (PMIP) simulations, Global and Planetary Change, 24, 79–106, 2000. 303, 311

Ramstein, G., Fabre, A., Pinot, S., Ritz, C., and Joussaume, S.: Ice-sheet mass balance during the Last Glacial Maximum, Ann. Glaciol., 25, 145–152, 1997. 303, 311

Raymo, M. E.: The timing of major climate terminations, Paleoceanography, 12, 577–585, 1997. 303

Raymo, M. E., Lisiecki, L. E., and Nisancioglu, K. H.: Plio-Pleistocene Ice Volume, Antarctica Climate, and the Global δ^{18}O Record, Science, 313, 492–495, 2006. 303

Reeh, N.: Parameterization of melt rate and surface temperature on the Greenland ice sheet, Polarforschung, 59, 113–128, 1991. 307

Climatic conditions for Northern Hemisphere ice sheets

A. Abe-Ouchi et al.

EGU

Ritz, C., Fabre, A., and Letréguilly, A.: Sensitivity of a Greenland ice sheet model to ice flow and ablation parameters: consequences for the evolution through the last climatic cycle, Clim. Dyn., 13, 11–24, 1997. 307

Roe, G. H. and Lindzen, R. S.: The Mutual Interaction between Continental-Scale Ice Sheets and Atmospheric Stationary Waves., J. Climate, 14, 1450–1465, 2001. 303

Saito, F. and Abe-Ouchi, A.: Thermal structure of Dome Fuji and east Dronning Maud Land, Antarctica, simulated by a three-dimensional ice-sheet model, Ann. Glaciol., 39, 433–438, 2004. 305, 306

Saito, F. and Abe-Ouchi, A.: Sensitivity of Greenland ice sheet simulation to the numerical procedure employed for ice sheet dynamics, Ann. Glaciol., 42, 331–336, 2005. 306

Saito, F., Abe-Ouchi, A., and Blatter, H.: An improved numerical scheme to compute horizontal gradients at the ice-sheet margin: its effect on the simulated ice thickness and temperature, Ann. Glaciol., 46, accepted, 2007. 319

Schlesinger, M. E. and Verbitsky, M.: Simulation of glacial onset with a coupled atmospheric general circulation/mixed-layer ocean-ice-sheet/asthenosphere model, Palaeoclimates–Data and Modelling, 2, 179–201, 1996. 303

Shinn, R. A. and Barron, E. J.: Climate Sensitivity to Continental Ice Sheet Size and Configuration, J. Climate, 2, 1517–1537, 1989. 303, 311

Svendsen, J. I., Alexanderson, H., Astakhov, V. I., Demidov, I., Dowdeswell, J. A., Funder, S., Gataullin, V., Henriksen, M., Hjort, C., Houmark-Nielsen, M., Hubberten, H. W., Ingolfsson, O., Jakobsson, M., Kjaer, K. H., Larsen, E., Lokrantz, H., Lunkka, J. P., Lysa, A., Mangerud, J., Matiouchkov, A., Murray, A., Moller, P., Niessen, F., Nikolskaya, O., Polyak, L., Saarnisto, M., Siegert, C., Siegert, M. J., Spielhagen, R. F., and Stein, R.: Late quaternary ice sheet history of northern Eurasia, Quat. Sci. Rev., 23, 1229–1271, 2004. 302

Tarasov, L. and Peltier, W. R.: Terminating the 100 kyr ice age cycle, J. Geophys. Res., 102, 21 665–21 693, 1997a. 303, 311

Tarasov, L. and Peltier, W. R.: A high-resolution model of the 100ka ice-age cycle, Ann. Glaciol., 25, 58–65, 1997b. 303, 307, 311

Tarasov, L. and Peltier, W.: Impact of thermomechanical ice sheet coupling on a model of the 100 kyr ice age cycle, J. Geophys. Res., 104, 9517–9546, 1999. 303, 311

Thompson, S. L. and Pollard, D.: Greenland and Antarctic Mass Balances for Present and Doubled Atmospheric CO_2 from the GENESIS Version-2 Global Climate Model, J. Climate, 10, 871–900, 1997. 303

Climatic conditions for Northern Hemisphere ice sheets

A. Abe-Ouchi et al.

Title Page

Abstract | Introduction

Conclusions | References

Tables | Figures

◄ | ►►

◄ | ►

Back | Close

Full Screen / Esc

Printer-friendly Version

Interactive Discussion

van de Wal, R. S. W.: Mass-balance modelling of the Greenland ice sheet: a comparison of an energy-balance and a degree-day model, Ann. Glaciol., 23, 36–45, 1996. 307

van den Berg, J., van de Wal, R. S. W., and Oerlemans, J.: Effects of spatial discretization in ice-sheet modelling using the shallow-ice approximation, J. Glaciol., 52, 89–98, 2006. 319

5 Verbitsky, M. Y. and Oglesby, R. J.: The effect of Atmospheric carbon dioxide concentration on continental glaciation of the northern hemisphere, J. Geophys. Res., 97, 5895–5909, 1992. 303

Yamagishi, T., Abe-Ouchi, A., Saito, F., Segawa, T., and Nishimura, T.: Re-evaluation of paleo-accumulation parameterization over Northern Hemisphere ice sheets during the ice age ex-

10 amined with a high-resolution AGCM and a 3-D ice-sheet model, Ann. Glaciol., 42, 433–440, 2005. 304, 305, 309, 313, 316, 317

Yokoyama, Y., Lambeck, K., De Deckker, P., Johnston, P., and Fifield, L. K.: Timing of the Last Glacial Maximum from observed sea-level minima, Nature, 406, 713–716, 2000.

Zweck, C. and Huybrechts, P.: Modeling of the northern hemisphere ice sheets during the

15 last glacial cycle and glaciological sensitivity, J. Geophys. Res., 110, D07103, doi:10.1029/2004JD005489, 2005. 304, 311, 319

Climatic conditions for Northern Hemisphere ice sheets

A. Abe-Ouchi et al.

EGU

Table 1. Boundary conditions for AGCM experiments. The terms E, O, P in Orbital conditions correspond to eccentricity, obliquity in degree, angular precession (longitude of perihelion) in degree, respectively. Orbital conditions and CO_2 content at 0 ka and LGM are E=0.01672, O=23.45, P=102.04, C=345 ppm; and E=0.018994, O=22.949, P=114.42, C=200 ppm, respectively, which are based on PMIP.

Experiment	Resolution	Ocean	Orbital condition			CO_2	Ice Sheet	
			E	O	P		extent	topography
CTLH	T106L20	0 ka SSTfix		0 ka		0 ka	0 ka	0 ka
LGMnice	T106L20	LGM SSTfix		LGM		LGM	0 ka	0 ka
LGMflat	T106L20	LGM SSTfix		LGM		LGM	LGM	0 ka
LGMfull	T106L20	LGM SSTfix		LGM		LGM	LGM	LGM
M21nice	T42L11	slab ocean		LGM		LGM	0 ka	0 ka
M21flat	T42L11	slab ocean		LGM		LGM	LGM	0 ka
M12nice	T42L11	slab ocean		LGM		LGM	12 ka	0 ka
M12flat	T42L11	slab ocean		LGM		LGM	12 ka	12 ka
M0CTL	T42L11	slab ocean		0 ka		0 ka	0 ka	0 ka
M21O1C1	T42L11	slab ocean	0.05	23.45	102.04	LGM	LGM	LGM
M21O1C2	T42L11	slab ocean	0.05	23.45	102.04	280 ppm	LGM	LGM
M21O1C3	T42L11	slab ocean	0.05	23.45	102.04	0 ka	LGM	LGM
M21O2C1	T42L11	slab ocean	0.05	23.45	282.	LGM	LGM	LGM
M21O2C3	T42L11	slab ocean	0.05	23.45	282.	0 ka	LGM	LGM
M0O1C2	T42L11	slab ocean	0.05	23.45	102.04	280 ppm	0 ka	0 ka
M0O2C2	T42L11	slab ocean	0.05	23.45	282.	280 ppm	0 ka	0 ka
M0O8C2	T42L11	slab ocean	0.	25.5	0.	280 ppm	0 ka	0 ka
M0O9C2	T42L11	slab ocean	0.	22.	0.	280 ppm	0 ka	0 ka

Title Page

Abstract   Introduction

Conclusions   References

Tables   Figures

|◄   ►|

◄   ►

Back   Close

Full Screen / Esc

Printer-friendly Version

Interactive Discussion

EGU

Table 2. Parameter choices for ice-sheet model experiments.

Parameter	A	B	C	Unit	Symbol
Lapse rate	−4.0	−5.0	−6.0	$\mathrm{K\,km^{-2}}$	λ in Eq. (9)
Desertification rate	0.01	0.022	0.04	–	d_0 in Eq. (11)
Albedo effect	−3.7	−4.7	−5.7	$10^{-13}\,\mathrm{K\,m^{-2}}$	γ_{area} in Eq. (10)

EGU
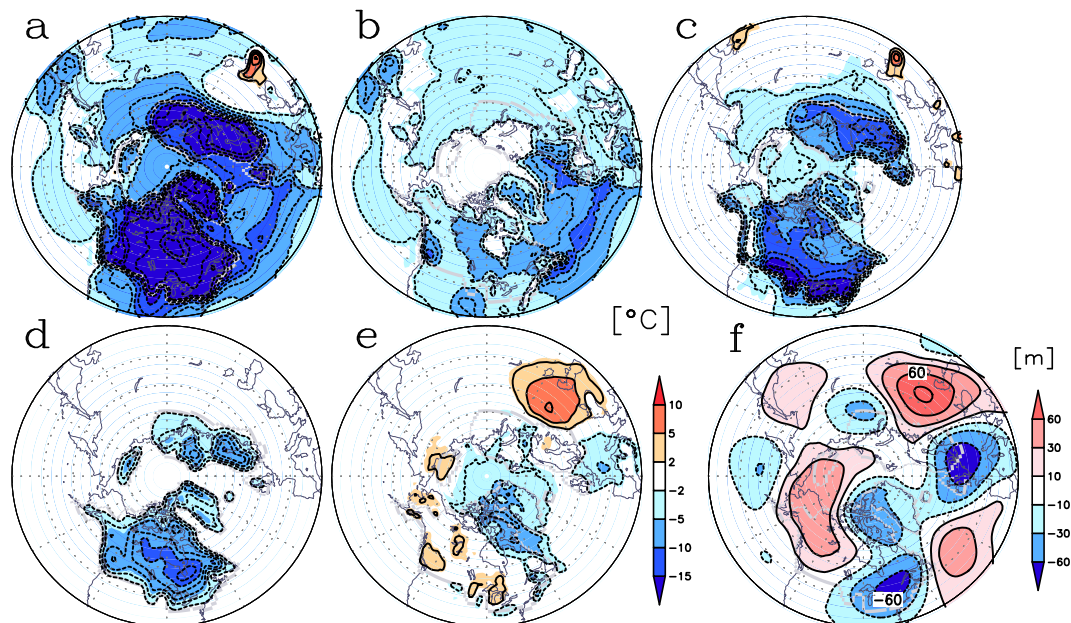
Fig. 1. Difference in summer surface air temperature (mean of June, July and August) in °C due to boundary conditions for **(a)** to **(e)**, and difference in summer geopotential height at 500 hPa level for (f). (a) Total difference by experiments (LGMfull−CTLH), **(b)** CO$_2$ and SST effect by experiments (LGMnice−CTLH), **(c)** Albedo effect by experiments (LGMflat−LGMnice), **(d)** Topography Lapse Rate Effect assuming a lapse rate 5 K km^{-1} for the given topography (LGMfull−LGMflat), **(e)** Topography effect other than the lapse rate effect as Residual (e=a−b−c−d). **(f)** Difference in summer geopotential height at 500 hPa level due to ice sheet topography (LGMfull−LGMflat). Contours of Figs. (a) to (e) are at: −50, −45, −35, −30, −25, −20, −17.5, −15, −12.5, −10, −7.5, −5, −2.5, 2.5, 5, 7.5, 10, 12.5. Contours of Fig. (f) are at: −150, −120, −90, −60, −30, −10, 10, 30, 60, 90, 120, 150. Gray line in the figures indicates the ice sheet extent used in the GCM.

Title Page

Abstract | Introduction

Conclusions | References

Tables | Figures

|◄ | ►|

◄ | ►

Back | Close

Full Screen / Esc

Printer-friendly Version

Interactive Discussion

EGU
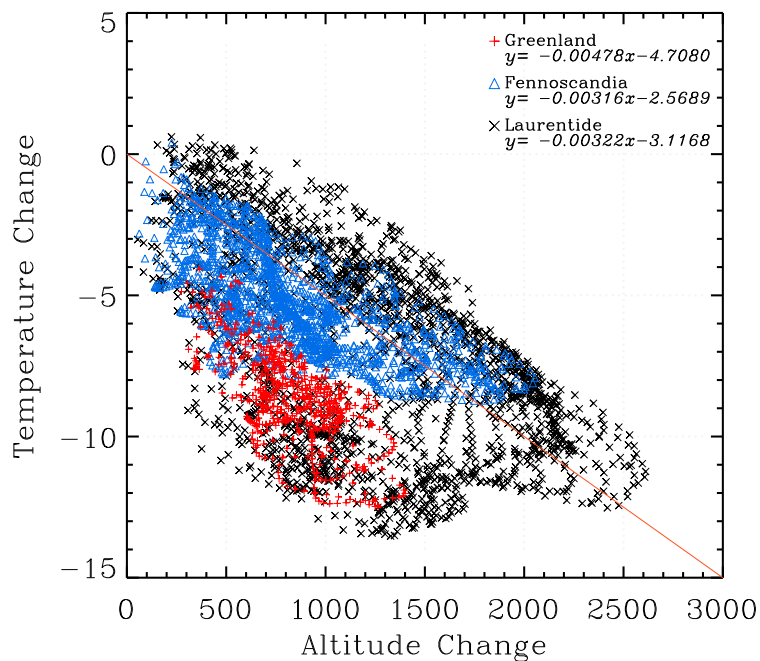
Fig. 2. Difference in summer surface temperature (mean of June, July and August) versus the difference in altitude for all the grid points over the ice sheet in the model. The red line corresponds to the relation of the lapse rate −5°C per 1 km. The red mark of scatter plots is for Greenland ice sheet, the blue mark for Fennoscandian ice sheet, and the black mark is for Laurentide ice sheet.
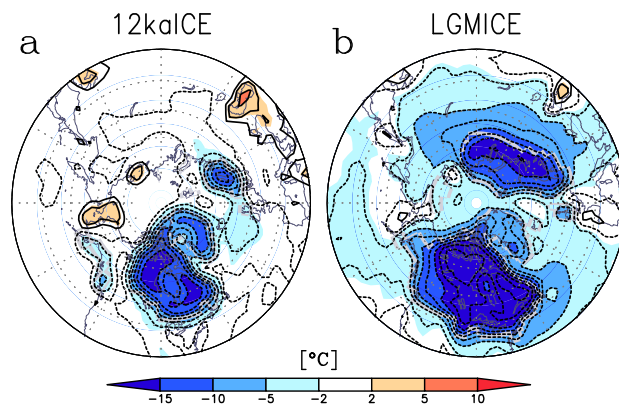
Fig. 3. Same as Fig. 1c, but for different sizes of "flat" ice sheet (at LGM and 12 ka). **(a)** M12flat−M21nice, **(b)** M21flat−M21nice.

EGU
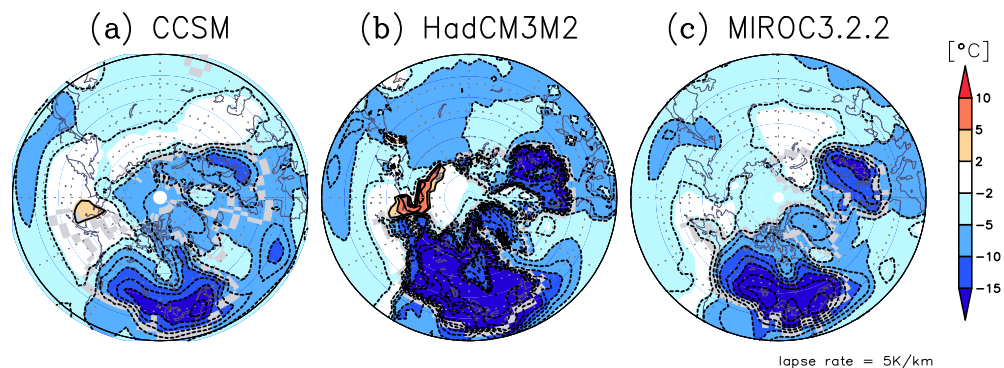
Fig. 4. Same as Fig. 1 but for PMIP2 models. **(a)** CCSM, **(b)** HadCM3M2, **(c)** MIROC3.2.2. Change in summer surface air temperature but the lapse rate effect (= $5\,\mathrm{K\,km^{-1}}$ for each modelled ice sheet topography) is extracted.

EGU
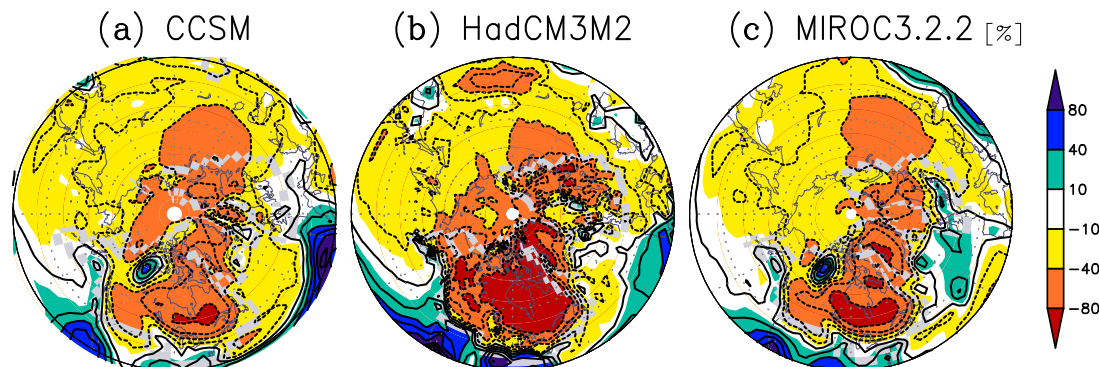
Fig. 5. Ratio of annual precipitation change in per cent for PMIP2 models: **(a)** CCSM, **(b)** HadCM3M2, **(c)** MIROC3.2.2 by using (LGM – CTL)/CTL. The contour interval is 20%.
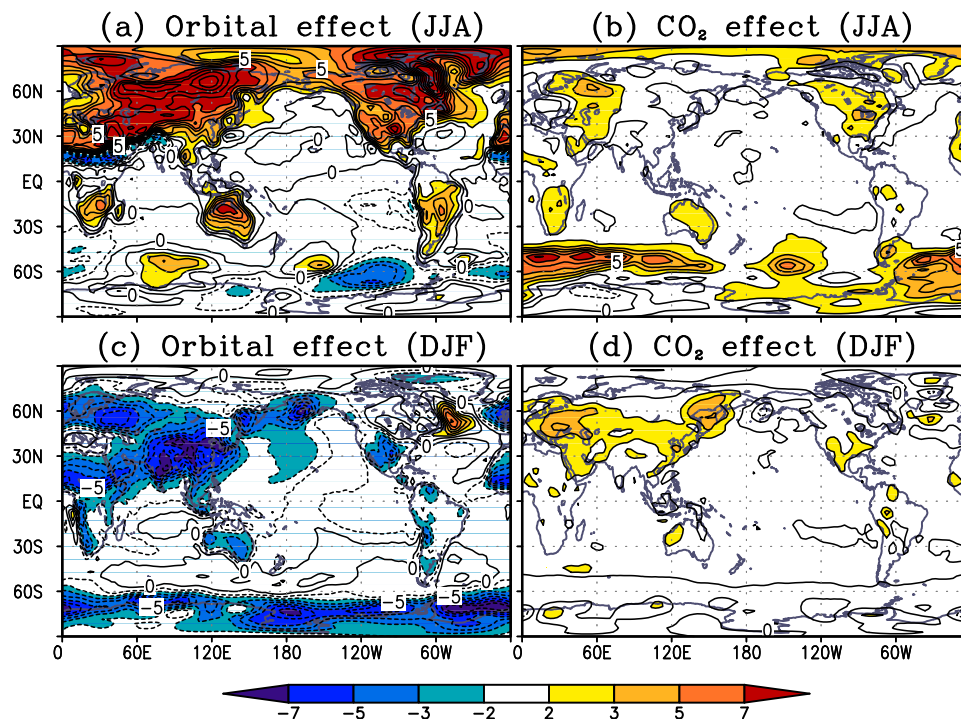
Fig. 6. Difference in the surface temperature of summer (mean of June, July, and August) and winter (mean of December, January, February) for two cases of different **(a)**, **(c)** Orbital effect and **(b)**, **(d)** CO_2 effect. Contour interval is 1˚C.

A686g [m]
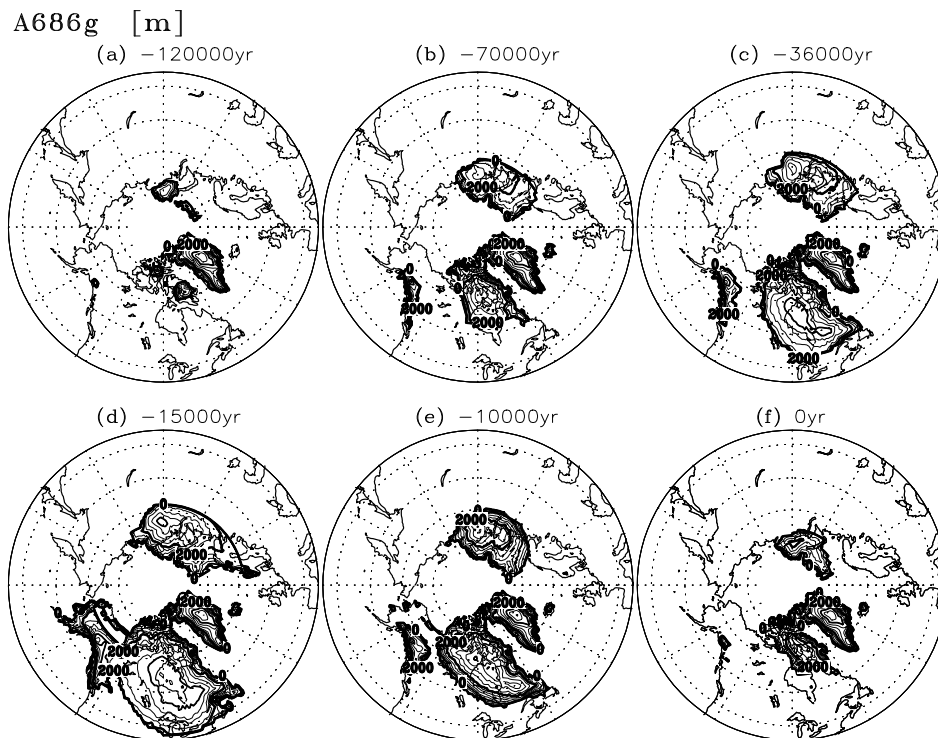
Fig. 7. Ice sheet distribution at different stages at **(a)** 120 ka, **(b)** 70 ka, **(c)** 36 ka, **(d)** 15 ka, **(e)** 10 ka, **(f)** 0 ka. Contour intervals are 250 m (thin), 1000 m (thick) and 2000 m (labeled). The volume of each ice sheet in terms of sea level contribution is (a) −6.278 m, (b) −51.643 m, (c) −90.253 m, (d) −137.827 m, (e) −77.167 m, (f) −27.095 m.
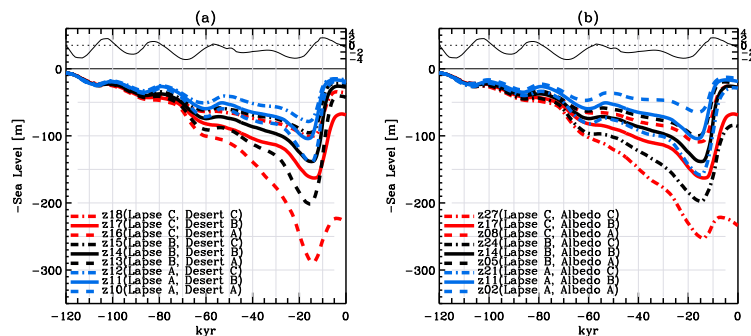
Fig. 8. Same as Fig. 7 but for the past 120 000 years and different cases depending on lapse rate, albedo-effect and desertification rate parameter. Lapse A $=4.0\,\mathrm{K\,km^{-1}}$, Lapse B $=5.0\,\mathrm{K\,km^{-1}}$, Lapse C $=6.0\,\mathrm{K\,km^{-1}}$; Desert A $=0.01$, Desert B $=0.022$, Desert C $=0.04$; Albedo A $=-3.7\times10^{-13}\,\mathrm{K\,m^{-2}}$, Albedo B $=-4.7\times10^{-13}\,\mathrm{K\,m^{-2}}$, Albedo C $=-5.7\times10^{-13}\,\mathrm{K\,m^{-2}}$. The lapse rate parameter corresponds to λ in Eq. (9). The desertification rate parameter corresponds to d_0 in Eq. (11). Albedo effect parameter corresponds to γ_{area} in Eq. (10).